Available online at www.sciencedirect.com
SCIENCE DIRECT
ELSEVIER
Journal of Magnetism and Magnetic Materials 300 (2006) 117–121
Journal of magnetism and magnetic materials
www.elsevier.com/locate/jmmm

Electromagnetic unidirectionality and frozen modes in magnetic photonic crystals

Alex Figotin, Ilya Vitebskiy*

University of California at Irvine, Irvine, CA 92697-3875, USA

Available online 14 November 2005

Abstract

Magnetic photonic crystals are periodic arrays of lossless materials, at least one of which being magnetically polarized. Magnetization, either spontaneous or induced, is associated with nonreciprocal effects, such as Faraday rotation. Magnetic photonic crystals of certain configuration can also display strong spectral asymmetry, implying that light propagates in one direction much faster or slower than in the opposite direction. This essentially nonreciprocal phenomenon can result in electromagnetic unidirectionality. A unidirectional medium, being perfectly transmissive for electromagnetic waves of certain frequency, freezes the radiation of the same frequency propagating in the opposite direction. The frozen mode has zero group velocity and drastically enhanced amplitude. The focus of our investigation is the frozen mode regime. Particular attention is given to the case of weak nonreciprocity, related to the infrared and optical frequencies. It appears that even if the nonreciprocal effects become vanishingly small, there is still a viable alternative to the frozen mode regime that can be very attractive for a variety of practical applications.

PACS: 78.20.Ls; 78.20.Bh; 41.20.Jb; 42.70.Qs; 42.65.Re

Keywords: Photonic crystals; Magneto-optics; Nonreciprocity; Slow light; Bianisotropic; Frozen light; Transmission resonance

1. Nonreciprocal effects in magnetic photonic crystals

In spatially periodic media, such as photonic crystals, the electromagnetic eigenmodes can be represented in the Bloch form

$$\Psi_k(\boldsymbol{r}+\boldsymbol{a}) = \Psi_k(\boldsymbol{r})\exp(\mathrm{i}\boldsymbol{k}\cdot\boldsymbol{a}), \tag{1}$$

where $\boldsymbol{k}$ is the Bloch wave vector and $\boldsymbol{a}$ is a lattice translation. The correspondence $\omega(\boldsymbol{k})$ between the Bloch wave vector $\boldsymbol{k}$ and the frequency ω is referred to as the dispersion relation. Due to spatial heterogeneity, the frequency band structure of a photonic crystal can be very complicated and it is essentially dependent on the geometry of the periodic array [1]. In most cases, though, the electromagnetic dispersion relation $\omega(\boldsymbol{k})$ remains strictly symmetric with respect to the change of the sign of the wave vector

$$\omega(\boldsymbol{k}) = \omega(-\boldsymbol{k}). \tag{2}$$

Indeed, all nonmagnetic photonic crystals support time reversal symmetry [2], which imposes the relation (2). In addition, the overwhelming majority of magnetic and nonmagnetic photonic crystals support space inversion symmetry, which also imposes the relation (2). Still, some magnetic photonic crystals have neither time reversal nor space inversion and can display electromagnetic spectral asymmetry

$$\omega(\boldsymbol{k}) \neq \omega(-\boldsymbol{k}), \tag{3}$$

which in some cases can be very significant [3,4]. There are two basic necessary conditions for strong spectral asymmetry in magnetic photonic crystals.

1. Magnetic component(s) of the composite structure must display significant circular birefringence (Faraday rotation) at the frequency range of interest.
2. The geometry of the periodic array must be complex enough so that its magnetic symmetry does not impose the relation (2).

*Corresponding author. Tel.: +1 949 824 7715; fax: +1 949 824 7993.
E-mail address: dvitebsk@math.uci.edu (I. Vitebskiy).

0304-8853/$ - see front matter © 2005 Elsevier B.V. All rights reserved.
doi:10.1016/j.jmmm.2005.10.046

The second condition imposes severe limitations on the periodic structure [3]. For example, a simplest periodic layered array supporting spectral asymmetry (3) must include at least three different layers in unite cell L, as shown in Fig. 1. Two of the layers (*A1* and *A2*) must have misaligned in-plane anisotropy with the misalignment angle φ different from 0 and $\pi/2$. An additional F layer must display significant Faraday rotation.

An important parameter of this structure is the misalignment angle $\varphi = \varphi_1 - \varphi_2$ between adjacent anisotropic layers A_1 and A_2. According to Ref. [3], the dispersion relation can become asymmetric only if the angle φ is different from 0 and $\pi/2$, as illustrated in Fig. 2.

Another critical parameter of the periodic array in Fig. 1 is the nonreciprocal circular birefringence g in the magnetic F layers. The spectral asymmetry (3) can be significant only in the case of strong Faraday rotation. If the magnitude g of Faraday rotation decreases, the degree of spectral asymmetry (3) also decreases and vanishes in the non-magnetic limiting case $g = 0$, as illustrated in Fig. 3. Note that the reciprocal circular birefringence occurring in nonmagnetic chiral media would never cause the spectral asymmetry (3). In other words, the presence of nonreciprocal magnetic components is essential.

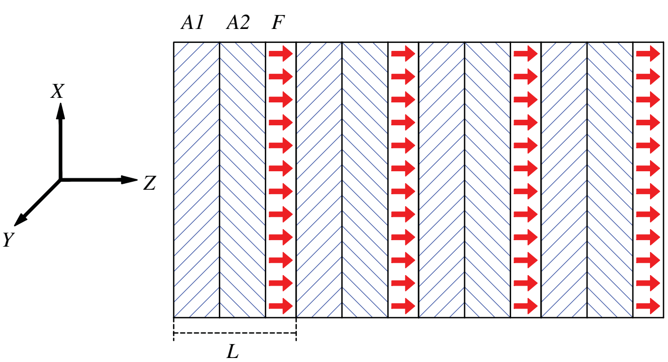

Fig. 1. A simplest periodic magnetic stack supporting asymmetric dispersion relation (3). A unit cell L includes a magnetic layer F with magnetization shown by the arrows, and two anisotropic dielectric layers A_1 and A_2 with different orientations φ_1 and φ_2 of the respective anisotropy axes in the x–y plane.

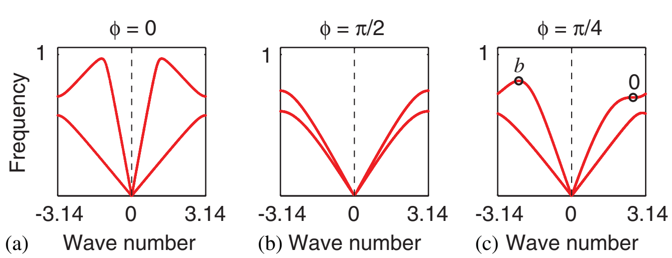

Fig. 2. Electromagnetic dispersion relation $\omega(k)$ of the periodic stack in Fig. 1 for three different values of the misalignment angle φ. Only the first frequency band is shown. In the cases $\varphi = 0$ (no misalignment) and $\varphi = \pi/2$, the dispersion relation is symmetric with respect to the sign of the Bloch wave vector $k \| z$.

The domain of definition of k in Fig. 3 is chosen between 0 and $2\pi/L$. Since the Bloch wave number is defined up to a multiple of $2\pi/L$, the graph in Fig. 3(d) is identical to that in Fig. 2(c).

2. Electromagnetic unidirectionality

Strong electromagnetic spectral asymmetry has various physical consequences, one of which is the effect of *unidirectional wave propagation*. Suppose that at $k = k_0$ and $\omega = \omega_0$ one of the spectral branches $\omega(k)$ develops a stationary inflection point

$$\frac{\partial \omega}{\partial k} = 0, \quad \frac{\partial^2 \omega}{\partial k^2} = 0, \quad \frac{\partial^3 \omega}{\partial k^3} \neq 0, \tag{4}$$

at $k = k_0$ and $\omega = \omega_0 = \omega(k_0)$, as shown in Figs. 3 and 4(a). At frequency $\omega = \omega_0$ in Fig. 4(a), there are two propagating Bloch waves: one with $k = k_0$ and the other with $k = k_1$. Only one of the two waves can transfer energy—the one with $k = k_1$ and negative group velocity. The Bloch eigenmode with $k = k_0$ has zero group velocity and does not contribute to the energy flux. This latter eigenmode is associated with stationary inflection point (4) and referred to as the *frozen mode*. At $\omega = \omega_0$, none of the Bloch modes has positive group velocity and, therefore, none of the Bloch modes can transfer the energy from left to right at this particular frequency. Thus, a photonic crystal with the dispersion relation similar to that in Fig. 4a, displays the property of *electromagnetic unidirectionality* at $\omega = \omega_0$.

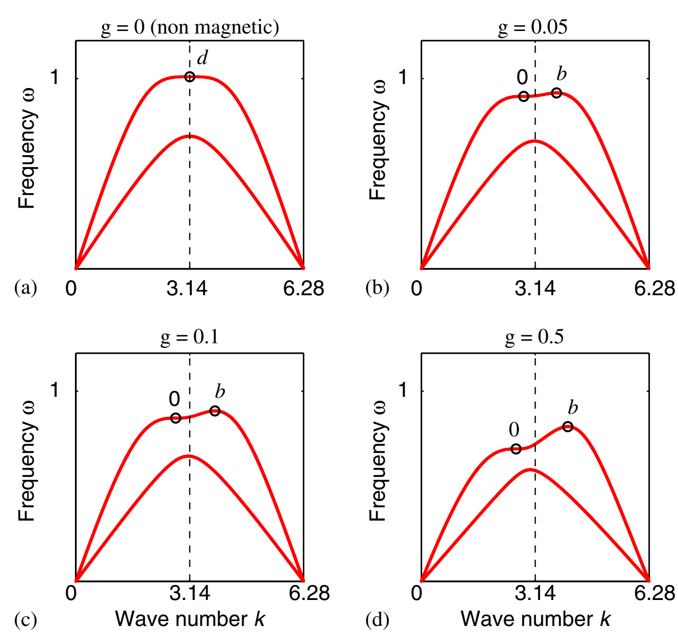

Fig. 3. Dispersion relation of the periodic stack in Fig. 1 for four different values of gyrotropy g. For any given g, the stack configuration is adjusted so that the dispersion curve $\omega(k)$ has a stationary inflection point 0, associated with the frozen mode regime. In the non-magnetic limit (a), the stationary inflection point 0 merges with the frequency band edge b and together they form a degenerate band edge d.

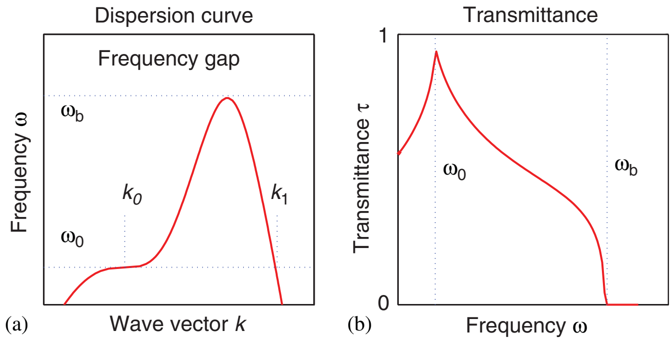

Fig. 4. (a) A fragment of asymmetric dispersion relation of the periodic stack in Fig. 1. At $k = k_0$, $\omega = \omega_0$ this spectral branch has stationary inflection point (4) associated with electromagnetic unidirectionality and the frozen mode. (b) Frequency dependence of the transmittance of semi-infinite photonic slab with the dispersion relation shown in Fig. 4(a). The incident light propagates from left to right, so the transmitted light inside the periodic array can propagate only in the positive direction along the z-axis. At the frequency ω_0 of stationary inflection point, the slab transmittance is close to unity, which implies that the incident wave is almost completely converted into the frozen mode with zero group velocity and drastically enhanced amplitude. At the band edge frequency ω_b, the semi-infinite photonic slab becomes totally reflective.

Such a remarkable effect can be viewed as an extreme manifestation of the spectral asymmetry (3).

Observe that the effect of unidirectionality does not require strong Faraday rotation in magnetic layers and strong spectral asymmetry. Indeed, even if the nonreciprocal effects are vanishingly small, the stack configuration can always be adjusted so that the stationary inflection point formally persists, as illustrated in Fig. 3. The problem though is that in such a case, the stationary inflection point moves very close to the nearest band edge b and, eventually, merges with it, as shown in Fig. 3(a). At this point the unidirectionality becomes virtually undetectable, because the forward and the backward waves become equally slow.

3. The frozen mode regime

Consider a plane electromagnetic wave incident from the left on a semi-infinite unidirectional photonic slab with the dispersion relation shown in Figs. 3(d) or 4(a). In the vicinity of stationary inflection point (4), the dispersion relation can be approximated as follows:

$$\omega = \omega_0 \approx \frac{\omega_0'''}{6}(k-k_0)^3, \quad \omega_0''' = \left(\frac{\partial^3\omega}{\partial k^3}\right)_{k=k_0}. \tag{5}$$

Inside the slab, the group velocity u of the respective propagating mode vanishes as ω approaches ω_0

$$u = \frac{\partial\omega}{\partial k} \approx \frac{1}{2}\omega_0'''(k-k_0)^2 \approx \frac{6^{2/3}}{2}(\omega_0''')^{1/3}(\omega-\omega_0)^{2/3}. \tag{6}$$

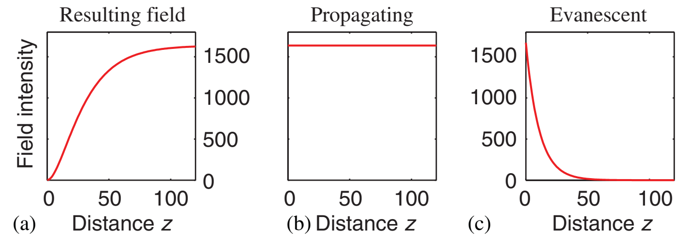

Fig. 5. Squared amplitude of the transmitted wave and its propagating and evanescent components inside semi-infinite stack in close proximity of the frozen mode frequency: (a) squared amplitude of the resulting field, (b) squared amplitude of the propagating field component, (c) squared amplitude of evanescent field component. The amplitude of the incident wave is unity. Due to destructive interference of the propagating and evanescent components, the resulting field at the slab/vacuum interface at $z = 0$ is small enough to satisfy the boundary conditions. The distance z from the slab boundary is expressed in units of L.

But remarkably, the electromagnetic energy density W associated with the transmitted frozen mode diverges as $\omega \to \omega_0$

$$W \approx \frac{2\tau S_I}{6^{2/3}}(\omega_0''')^{-1/3}(\omega-\omega_0)^{-2/3}, \tag{7}$$

where S_I is the fixed energy flux of the incident wave. Transmittance/reflectance coefficients of lossless semi-infinite slab are defined as

$$\tau = \frac{S_T}{S_I}, \quad \rho = -\frac{S_R}{S_I} = 1 = \tau, \tag{8}$$

where S_R and S_T are the energy fluxes of the reflected and transmitted waves, respectively. Transmittance τ remains finite at $\omega = \omega_0$, as illustrated in Fig. 4(b). Thus, the energy flux

$$S_T = \tau S_I = uW \tag{9}$$

of the transmitted frozen mode also remains finite at $\omega = \omega_0$ and can even be close to that of the incident wave [4]. The latter implies that the incident light gets trapped inside the unidirectional slab in the form of coherent frozen mode with infinitesimal group velocity (6) and diverging energy density (7).

Electromagnetic field distribution inside the photonic slab in close proximity of the frozen mode frequency ω_0 is shown in Fig. 5(a).

According to Eq. (7), the saturation field intensity inside the periodic medium diverges as ω approaches ω_0. In reality, though, the frozen mode amplitude will always be limited by such factors as absorption, nonlinear effects, imperfection of the periodic array, deviation of the incident radiation from a perfect plane monochromatic wave, finiteness of the photonic slab dimensions, etc. Still, with all these limitations in place, the frozen mode regime can be very attractive for various applications.

4. Frozen mode regime at the degenerate photonic band edge

The frozen mode regime and the electromagnetic unidirectionality are both associated with stationary inflection point (4) on the k–ω diagram. In the case of normal incidence of light on a periodic layered structure, the two phenomena always coexist [4–6], although the frozen mode regime per se is not a nonreciprocal effect, while the electromagnetic unidirectionality is. At optical frequencies, all nonreciprocal effects, including magnetic gyrotropy, become too weak to support an appreciable spectral asymmetry (3). As a consequence, a stationary inflection point of the dispersion curve can only develop in a very close proximity to the photonic band edge. Let us see what happens in the important limiting case of $g \to 0$, where the stationary inflection point 0 merges with the band edge b and together, they form a degenerate band edge d, as shown in Fig. 3(a). In the vicinity of the degenerate band edge d, the dispersion curve $\omega(k)$ can be approximated as

$$\omega_d - \omega \approx \frac{\omega_d''''}{24}(k-k_d)^4, \quad \omega_d'''' = \left(\frac{\partial^4\omega}{\partial k^4}\right)_{k=k_d} < 0. \tag{10}$$

The group velocity u of the respective propagating mode vanishes as ω approaches ω_d

$$u = \frac{\partial\omega}{\partial k} \approx \frac{\omega_d''''}{6}(k-k_d)^3 \approx \frac{24^{3/4}}{6}(\omega_d'''')^{1/4}|\omega_d - \omega|^{3/4} \quad \text{at } \omega \leqslant \omega_d, \tag{11}$$

while the light intensity W associated with the transmitted frozen mode diverges

$$W \propto |\omega_d - \omega|^{-1/2} \quad \text{at } \omega \leqslant \omega_d. \tag{12}$$

The divergence (12) is slightly weaker than in the case (7) of stationary inflection point. But in either case, Fig. 5 provides a good graphic illustration of the electromagnetic field distribution inside the slab in the vicinity of the respective stationary point 0 or d.

As the frequency ω approaches ω_d, both the propagating and the evanescent Bloch contributions to the transmitted wave grow sharply, while remaining nearly equal and opposite in sign at the slab boundary. Yet, there is a crucial difference between the two cases. Eq. (11) together with (12) yield that in spite of huge and diverging amplitude (12) of the transmitted frozen mode, the corresponding energy flux S_T vanishes as ω approaches ω_d

$$S_T = Wu \propto \begin{cases} (\omega_d - \omega)^{1/4} & \text{at } \omega \leqslant \omega_d, \\ 0 & \text{at } \omega \geqslant \omega_d. \end{cases}$$

By contrast, in the vicinity of stationary inflection point, the slab transmittance τ remains finite even at $\omega = \omega_0$, and so does the energy flux (9) associated with the frozen mode.

The situation at degenerate band edge can be viewed as an intermediate between the frozen mode regime at stationary inflection point and the vicinity of a regular band edge. Indeed, on the one hand, the incident wave at $\omega = \omega_d$ is totally reflected back to space, as would be the case at a regular photonic band edge. On the other hand, the field intensity (12) inside the slab becomes huge as $\omega \to \omega_d$, which is similar to what occurs at the frequency of stationary inflection point (4). In fact, an incident pulse with the central frequency close to the degenerate band edge ω_d, is transmitted inside the photonic slab, where it forms the frozen mode with drastically enhanced amplitude. But then, contrary to the case (4) of stationary inflection point, the frozen mode does not propagate through the slab and instead is reflected back to space. The large amplitude of the transmitted frozen mode at $\omega \approx \omega_d$ can be very attractive for a variety of applications, given the fact that this effect persists even in the case of vanishingly small Faraday rotation.

Although a degenerate band edge d can occur even in perfectly reciprocal periodic layered media, still some symmetry requirement should be met. For example, in the case of a periodic stack in Fig. 1, the existence of a degenerate photonic band edge requires misaligned in-plane anisotropy in the adjacent A–layers, with the misalignment angle φ being different from 0 and $\pi/2$. The proof can be found in Ref. [7,8].

5. Frozen mode regime in finite photonic crystals

Up to this point we only considered light incident on the surface of a semi-infinite photonic crystal. Since real structures are always bounded, the question arises whether and how the photonic crystal boundaries affect the frozen mode regime. In this section we outline several different scenarios.

5.1. Thick photonic slab

The spatial length l of a pulse inside unbounded photonic crystal

$$l \sim l_0 u/c, \tag{13}$$

where l_0 is the spatial length of the same pulse in vacuum, and u is the group velocity of light in the periodic medium. The quantity l_0 is directly related to the pulse bandwidth $\Delta\omega$

$$\Delta\omega/\omega \sim \lambda_0/l_0 = 2\pi c(\omega l_0)^{-1}, \tag{14}$$

where $\lambda_0 = 2\pi/\omega$ is the wavelength in vacuum. If instead of an infinite photonic crystal we have a bounded photonic slab of thickness D, the simple interpretation of the group velocity u as the speed of pulse propagation can still apply, provided that the space length l of the pulse inside the photonic slab is much smaller than the slab itself

$$l \ll D. \tag{15}$$

Taking into account the relations (13) and (14), the condition (15) can also be recast as a lower limit on the pulse bandwidth

$$\Delta\omega \gg 2\pi u/D, \tag{16}$$

implying that in order to fit inside the slab, the pulse should not have too narrow bandwidth.

In the vicinity of the frozen mode regime, the group velocity u decreases sharply, and so does the pulse length l in (13). The so compressed slow pulse with fixed bandwidth $\Delta\omega$ is more likely to fit inside the finite photonic crystal, compared to a fast pulse with the same bandwidth. The slower the pulse is, the better the condition (15) or (16) is satisfied. If a pulse satisfying the condition (15) or (16) is incident on a finite photonic slab, the slab can be treated as a semi-infinite medium until the pulse actually hits the opposite boundary of the slab.

5.2. Thin photonic slab

A qualitatively different picture emerges if the pulse length l defined in (13) is comparable in magnitude or exceeds the photonic slab thickness D. In such a case, the photonic slab is too thin to accommodate the entire pulse. Hence, at frequencies below the photonic band edge, the electromagnetic field inside the slab becomes a superposition of forward and backward propagating waves undergoing multiple reflections from two opposite boundaries of the slab. This situation by no means can be interpreted as an individual pulse propagating through the periodic medium, because at any moment of time the electromagnetic field inside the slab cannot be viewed as a wave packet built around a single propagating mode. The terms "slow light" or "frozen mode" do not literally apply here. Yet, it would be appropriate to discuss briefly what happens if the photonic slab becomes too thin to be treated as a semi-infinite periodic structure.

Assume that the photonic slab is thin enough to satisfy the inequality

$$l \gg D, \tag{17}$$

which is opposite to Eq. (15). The condition (17) establishes an upper limit on the incident pulse bandwidth

$$\Delta\omega \ll 2\pi u/D,$$

which includes the case of monochromatic incident light (the steady-state regime). If the photonic slab is lossless, its steady-state transmittance displays sharp transmission peaks associated with the so-called transmission band edge resonances, also known as Fabry-Perot cavity resonances. Such resonances are accompanied by a dramatic enhancement of the field intensity inside the slab. Commonly, this enhancement is proportional to N^2, where N is the number of layers in the stack. But in the case of degenerate band edge d, the field enhancement appears to be much stronger and is proportional to N^4. The detailed analysis of this spectacular effect can be found in [8].

Note that the Fabry–Perot cavity resonance in a finite photonic structure is qualitatively different from the frozen mode regime. The former is extremely sensitive to the slab thickness and the incident light bandwidth, it can occur only at frequencies lying within the transmission band.

The analysis based on the relations (13)–(17) is not applicable to the frozen mode regime at the frequency of degenerate band edge. Indeed, at $\omega \geqslant \omega_d$, the photonic crystal is totally reflective, and any reference to a light pulse propagating through the periodic medium is irrelevant. Still, even in this case, the slab thickness, along with absorption and nonlinearity, are fundamental limiting factors for the frozen mode amplitude.

Acknowledgements

The effort of A. Figotin and I. Vitebskiy was supported by the US Air Force Office of Scientific Research under the Grant FA9550-04-1-0359.

References

[1] J. Joannopoulos, R. Meade, J. Winn, Photonic Crystals, Princeton, 1995.
[2] L.D. Landau, et al., Electrodynamics of Continuous Media, Pergamon, New York, 1984.
[3] A. Figotin, I. Vitebsky, Phys. Rev. E 63 (2001) 066609.
[4] A. Figotin, I. Vitebskiy, Phys. Rev. B 67 (2003) 165210.
[5] A. Figotin, I. Vitebskiy, Phys. Rev. E 68 (2003) 036609.
[6] J. Ballato, A. Ballato, A. Figotin, I. Vitebskiy, Phys. Rev. E 71 (2005) 036612.
[7] A. Figotin, I. Vitebskiy, Waves in Random and Complex Media, submitted (arXiv:physics/0504112 v2 19 Apr 2005).
[8] A. Figotin, I. Vitebskiy, Phys. Rev. E 72 (2005) 036619.